JOC*Article*

Clar Goblet and Related Non-Kekulé Benzenoid LPAHs. A Theoretical Study

Sergey Pogodin and Israel Agranat*

Department of Organic Chemistry, The Hebrew University of Jerusalem, Jerusalem 91904, Israel

isria@vms.huji.ac.il

Received November 20, 2002

The results of an ab initio and semiempirical study of Clar Goblet (**1**), a $C_{38}H_{18}$ non-Kekulé diradical LPAH, and its constitutional isomers **4** and **5** are reported. Planar D_{2h}-**1** was only 87.4 (triplet) and 83.8 (singlet) kJ/mol less stable than its planar Kekulé isomer C_{2v}-**6** (at (U)B3LYP/6-31G*). Planar C_s-**4** was 63.6 (triplet) and 76.5 (singlet) kJ/mol less stable than **6**. Overcrowded C_1-**5** was 80.1 (triplet) and 98.1 (singlet) kJ/mol less stable than **6**. In concealed non-Kekulé **1**, the singlet was more stable then the triplet by 3.6 kJ/mol, while in nonconcealed non-Kekulé **4** and **5**, the triplets were more stable than the corresponding singlets by 12.9 and 18.1 kJ/mol, respectively, in accordance with theory. The spin density in **1**, **4**, and **5** is delocalized throughout the positions corresponding to active *peri*−*peri* coupling positions of the radical anion of naphthanthrone (**2**). The bond lengths in **1**, **4**, and **5** are in the range expected for aromatic compounds, except for the central carbon−carbon bonds, which are considerably elongated. A certain stabilization is evident in the homodesmotic reaction singlet-**1** + **10** + **10** → **11** + **3** + **3**, indicating a "communication" between the two benzo[*cd*]pyrenyl radical (**3**) units of diradical **1**. The HOMA indices indicate that in both singlet **1** and triplet **1** all of the rings except the central one have a significant aromatic character. The central ring is essentially antiaromatic, having negative HOMA index (−0.140 at UB3LYP/6-31+G*). The stabilities of $\mathbf{1}^{2-}$ and $\mathbf{1}^{2+}$ are decreased relative to $\mathbf{3}^{-}$ and $\mathbf{3}^{+}$, respectively.

Introduction

In 1972, Clar predicted that the $C_{38}H_{18}$ large polycyclic aromatic hydrocarbon (LPAH)[1] 4*H*,13*H*-diphenaleno-[2,1,9,8-*defg*:2′,1′,9′,8′-*opqr*]pentacene-4,13-diyl (dianthra-[1,9,8-*bcde*:1′,9′,8′-*klmn*]perylene) (D_{2h}-**1**) should exist and raised the possibility that it would be synthesized and would be found to be stable.[2] Clar's experiments to synthesize **1** by reductive dimerization of 6*H*-benzo[*cd*]-pyren-6-one (naphthanthrone, **2**), through *peri*−*peri* coupling, under conditions of the Clar synthesis (Zn, NaCl/$ZnCl_2$ melt, 300°) had been unsuccessful.[3] We have previously claimed that this attempted synthesis of **1** was a priori doomed, in view of the following arguments.[4] The peropyrene-type reductive dimerization of **2** requires the formation of the radical anion of **2** (**2a**) as an intermediate. The high spin density in **2a** is delocalized throughout positions 2, 3, 5, 6, 7, 9, 10, and 11a, while the spin densities at the remaining *peri* positions 1 and 11 were expected to be negligible. This was inferred from the coloring of the vertices of **2a**. When the C^6 vertex is black, then C^2, C^3, C^5, C^7, C^9, and C^{10} are black, while C^1, C^4, C^8, and C^{11} are white. Thus, any carbon−carbon coupling of two radical anions **2a** necessarily excludes C^1 and/or C^{11} as the sites of coupling. This analysis was supported by the McLahlan spin densities in benzo[*cd*]pyrenyl radical (**3**).[5] It was not surprising, therefore, that the [1,11] pair was inactive in the carbon−carbon coupling and consequently the [1,11]-[1′,11′] *peri*−*peri* coupling of **2** could not be realized.[4] For similar reasons, the isomeric LPAHs 4*H*,11*H*-anthra[8,9,1,2-*cdefg*]phenaleno[2,1,9,8-*opqr*]pentacene-4,11-diyl (C_s-**4**) and 4*H*,15*H*-benzo[*jk*]-

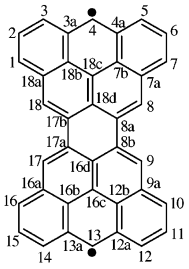

1

Clar Goblet

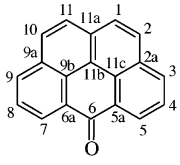

2

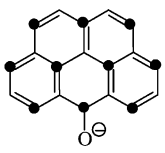

2a

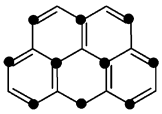

3

(1) Fetzer, J. C. *Large (C ≥ 24) Polycyclic Aromatic Hydrocarbons: Chemistry and Analysis*; Wiley-Interscience: New York, 2000.
(2) Clar, E. *The Aromatic Sextet*; Wiley: London, 1972; p 119.
(3) Clar, E.; Mackay, C. C. *Tetrahedron* **1972**, *28*, 6041−6047.
(4) Agranat, I.; Suissa, M. R. *Polycyclic Aromat. Compd.* **1992**, *3*, 51−61.
(5) Lewis, I. C.; Singer, L. S. *Magn. Reson. Chem.* **1985**, *23*, 698−704.

10.1021/jo026741v CCC: $25.00
Published on Web 03/12/2003

naphtho[2,1,8,7-*opqr*]phenaleno[2,1,9,8-*defg*]pentacene-4,15diyl (C_1-**5**) could not be formed by [1,11]-[2′,3′] and [1,11]-[5′,6′] couplings of **2**, respectively.[4]

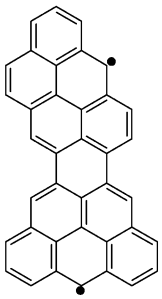

4

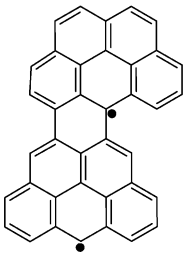

5

Clar's beautiful target molecule **1**[6a,7] is a non-Kekulé molecule, i.e., a molecule that is fully conjugated, but each of whose Kekulé structures contains at least two atoms that are not π-bonded.[8−11] A distinction has been made between concealed and nonconcealed (obvious) non-Kekulé hydrocarbons.[6a,7,12,13] In a concealed non-Kekulé hydrocarbon, the number of starred carbon vertices is equal to the number of unstarred carbon vertices, leading to the same number of peaks and valleys.[13] LPAH **1** is a concealed non-Kekulé hydrocarbon;[6a,7] it belongs to the smallest class of concealed non-Kekulé benzenoid PAHs, with 11 hexagons. It has been shown that there are eight members in this class, but only one with D_{2h} symmetry (molecule **1**). The other members of the class, which contain overcrowded regions cove and/or fjord,[6b] are expected to be nonplanar.[7b] LPAH **1** was referred to as "Clar Goblet" in a review entitled "The hunt for concealed non-Kekuléan polyhexes".[14] It has also been described as an hourglass-shaped hydrocarbon, having an isthmus.[15] It is surprising that Clar Goblet has attracted only limited computational attention. It has been predicted that **1**, being a diradical, may well exist in a singlet state or have a nearly degenerate singlet/triplet ground state, is "essentially disconnected", and might be regarded as being nearly a "closed-shell system" with number of resonance structures $SC = 2704$ (SC(**1**) = [SC(benzo[*cd*]-pyrene (**3**))]^2).[15] Recently we have reported the results of a semiempirical study and an ab initio study of Kekulé benzenoid LPAHs, isomers of **1**, potential LPAH $C_{38}H_{18}$ products of *peri*−*peri* reductive couplings of naphthanthrone (**2**), with emphasis on the overcrowding motif.[16,17]

Contrary to LPAHs **1**, its constitutional isomers **4** and **5** are nonconcealed non-Kekulé hydrocarbons, i.e., the numbers of starred and unstarred carbon vertices are unequal. The former (**4**) is planar, whereas the latter (**5**) is nonplanar as a result of the overcrowding at the cove region. LPAHs **4** and **5** are both unknown. We report here the results of an ab initio unrestricted HF, DFT, and MP2 study of the non-Kekulé LPAHs **1**, **4**, and **5** with special emphasis on Clar Goblet. The results of semiempirical calculations of **1**, **4**, and **5** using the AM1 and PM3 methods are also included.

Methods

The programs Gaussian94[18] and Gaussian98[19] were used for Hartree−Fock (HF), Density Functional Theory (DFT), and second-order Møller−Plesset perturbation theory (MP2) ab initio calculations. The RHF Hamiltonian was used for the closed shell systems **6**−**8**, and the UHF Hamiltonian was used for the singlet and triplet states of **1**, **4**, and **5**. Becke's three-parameter hybrid density functional B3LYP,[20] with the nonlocal correlation functional of Lee, Yang, and Parr[21−23] was used. The basis sets STO-3G, 6-31G*, 6-31+G*, and 6-311G** were employed. MP2 single-point calculations were carried out at the HF/6-31G* optimized geometries. All structures were fully optimized using symmetry constraints as indicated. Frequencies were calculated to verify minima at the B3LYP/STO-3G or B3LYP/6-31G* optimized structures of the systems under study. Program GaussView2.0[24] was used to visualize the results of ab initio calculations. The semiempirical calculations were performed using the AM1 and PM3 methods with Multi-electron Configuration Interaction calculations, as imple-

(6) (a) Gutman, I.; Cyvin, S. J. *Introduction to the Theory of Benzenoid Hydrocarbons*; Springer-Verlag: Berlin, 1989; pp 62−66; (b) pp 20−25.
(7) (a) Cyvin, S. J.; Gutman, I. *Kekulé Structures in Benzenoid Hydrocarbon (Lecture Notes in Chemistry 46)*; Springer-Verlag: Berlin, 1988; pp 18−23 and 51−58. (b) Cyvin, B. N.; Brunvoll, J.; Cyvin, S. J. In *Topics in Current Chemistry 162, Advances in the Theory of Benzenoid Hydrocarbons II*; Gutman, I., Ed.; Springer-Verlag: Berlin 1992; pp 140−143.
(8) Longuet-Higgins, H. C. *J. Chem. Phys.* **1950**, *18*, 265−274.
(9) Dewar, M. J. S. *The Molecular Orbital Theory of Organic Chemistry*; McGraw-Hill Book Company: New York, 1969; p 232.
(10) Borden, W. T.; Iwamura, H.; Berson, J. A. *Acc. Chem. Res.* **1994**, *27*, 109−116.
(11) Minkin, V. I. Glossary of Terms Used in Theoretical Organic Chemistry (IUPAC Recommendations 1999). *Pure Appl. Chem.* **1999**, *71*, 1919−1981.
(12) Gutman, I. *Croat. Chem. Acta* **1974**, *46*, 209−215.
(13) Cyvin, S. J.; Gutman, I. *J. Mol. Struct. (THEOCHEM)* **1987**, *150*, 157−169.
(14) Cyvin, S. J.; Brunvoll, J.; Cyvin, B. N. *J. Math. Chem.* **1990**, *4*, 47−54.
(15) Dias, J. R. *Phys. Chem. Chem. Phys.* **1999**, *1*, 5081−5086.
(16) Pogodin, S.; Agranat, I. *Polycyclic Aromat. Compd.* **2001**, *18*, 247−263.
(17) Pogodin, S.; Agranat, I. *J. Org. Chem.* **2002**, *67*, 265−270.
(18) Frisch, M. J.; Trucks, G. W.; Schlegel, H. B.; Gill, P. M. W.; Johnson, B. G.; Robb, M. A.; Cheeseman, J. R.; Keith, T.; Petersson, G. A.; Montgomery, J. A.; Raghavachari, K.; Al-Laham, M. A.; Zakrzewski, V. G.; Ortiz, J. V.; Foresman, J. B.; Cioslowski, J.; Stefanov, B. B.; Nanayakkara, A.; Challacombe, M.; Peng, C. Y.; Ayala, P. Y.; Chen, W.; Wong, M. W.; Andres, J. L.; Replogle, E. S.; Gomperts, R.; Martin, R. L.; Fox, D. J.; Binkley, J. S.; Defrees, D. J.; Baker, J.; Stewart, J. P.; Head-Gordon, M.; Gonzalez, C.; Pople, J. A. *Gaussian 94*, revision E.2; Gaussian, Inc.: Pittsburgh, PA, 1995.
(19) Frisch, M. J.; Trucks, G. W.; Schlegel, H. B.; Scuseria, G. E.; Robb, M. A.; Cheeseman, J. R.; Zakrzewski, V. G.; Montgomery, J. A., Jr.; Stratmann, R. E.; Burant, J. C.; Dapprich, S.; Millam, J. M.; Daniels, A. D.; Kudin, K. N.; Strain, M. C.; Farkas, O.; Tomasi, J.; Barone, V.; Cossi, M.; Cammi, R.; Mennucci, B.; Pomelli, C.; Adamo, C.; Clifford, S.; Ochterski, J.; Petersson, G. A.; Ayala, P. Y.; Cui, Q.; Morokuma, K.; Malick, D. K.; Rabuck, A. D.; Raghavachari, K.; Foresman, J. B.; Cioslowski, J.; Ortiz, J. V.; Baboul, A. G.; Stefanov, B. B.; Liu, G.; Liashenko, A.; Piskorz, P.; Komaromi, I.; Gomperts, R.; Martin, R. L.; Fox, D. J.; Keith, T.; Al-Laham, M. A.; Peng, C. Y.; Nanayakkara, A.; Gonzalez, C.; Challacombe, M.; Gill, P. M. W.; Johnson, B.; Chen, W.; Wong, M. W.; Andres, J. L.; Gonzalez, C.; Head-Gordon, M.; Replogle, E. S.; Pople, J. A. *Gaussian 98*, revision A.7; Gaussian, Inc.: Pittsburgh, PA, 1998.
(20) Becke, A. D. *J. Chem. Phys.* **1993**, *98*, 5648−5652.
(21) Lee, C.; Yang, W.; Parr, R. G. *Phys. Rev. B* **1988**, *37*, 785−789.
(22) Miehlich, B.; Savin, A.; Stoll, H.; Preuss, H. *Chem. Phys. Lett.* **1989**, *157*, 200−206.
(23) Vosko, S. H.; Wilk, L.; Nusair, M. C*an. J. Phys.* **1980**, *58*, 1200−1211.
(24) *GaussView* Rev. 2.08; copyright 2002 Gaussian, Inc; copyright 1998 Semichem, Inc.

TABLE 1. Semiempirical AM1 and PM3 Relative Enthalpies of Formation $\Delta\Delta H_f°$ (kJ/mol) of the LPAHs 1, 4−6

		symmetry		AM1 calculations				PM3 Calculation			
				C.I. = 2[c]	C.I. = 4[c]	C.I. = 6[c]	C.I. = 8[c]	C.I. = 2[c]	C.I. = 4[c]	C.I. = 6[c]	C.I. = 8[c]
1	**pl**[a]	D_{2h}	T[b]	96.53	100.93	104.50	86.10	96.77	101.12	103.74	86.80
1	**pl**	D_{2h}	S	96.50	95.07	98.23	88.96	96.73	95.61	104.28	89.10
4	**pl**	C_s	T	87.62	83.08	82.35	79.44	88.82	84.58	84.67	81.30
4	**pl**	C_s	S	104.11	102.14	105.27	101.63	103.65	102.11	103.91	101.01
5	**tf**	C_1	T	87.00	88.43	85.41	76.58	94.97	96.33	93.18	84.64
5	**tf**	C_1	S	121.83	123.58	129.12	116.96	128.83	130.71	135.13	123.94
6	**pl**	C_{2v}	S	0.00	0.00	0.00	0.00	0.00	0.00	0.00	0.00

[a] **pl**: planar conformation, **tf**: twisted-folded conformation. [b] S: singlet, T: triplet. [c] 2, 4, 6, or 8 molecular orbitals respectively were used in Configuration Interaction calculations.

TABLE 2. Ab Initio Relative Energies ΔE_{Tot} (kJ/mol) of LPAHs 1, 4−8

		symmetry			UHF/6-31G*	UB3LYP/STO-3G	UB3LYP/6-31G*	UB3LYP/6-311G**	UMP2/6-31G*//UHF/6-31G*
1	**pl**[a]	D_{2h}	T[b]	M[c]	−209.61	81.65	87.40	90.37	767.27
1	**pl**	D_{2h}	S	M	−318.18	76.36	83.80	86.93	798.40
4	**pl**	C_s	T	M		56.46	63.63		
4	**pl**	C_s	S	M		72.41	76.52		
5	**tf**	C_1	T	M		70.40	80.05		
5	**tf**	C_1	S	M		94.83	98.14		

					RHF/6-31G*	RB3LYP/STO-3G	RB3LYP/6-31G*	RB3LYP/6-311G**	RMP2/6-31G*//RHF/6-31G*
6	**pl**	C_{2v}	S	M	0.00	0.00	0.00	0.00	0.00
7	**pl**	C_{2h}	S	M	14.93	8.66	8.34	8.44	
8	**tf**	C_2	S	M	−4.29	−8.09	5.47	6.43	

[a] **pl**: planar conformation, **tf**: twisted-folded conformation. [b] S: singlet, T: triplet. [c] M: minimum (no imaginary frequencies, at B3LYP/STO-3G).

mented in the program MOPAC 93.[25,26] The geometries of all LPAHs were fully optimized using the keywords AM1 (or PM3) EF PRECISE KING SYMMETRY GNORM = 1 LET DDMIN = 0 MECI C.I. = 2, 4, 6, or 8 (up to 121 lowest microstates were used in MECI) OPEN(2,2) (for LPAHs **1**, **4**, and **5**) ESR (for the triplet states of **1**, **4**, and **5**).

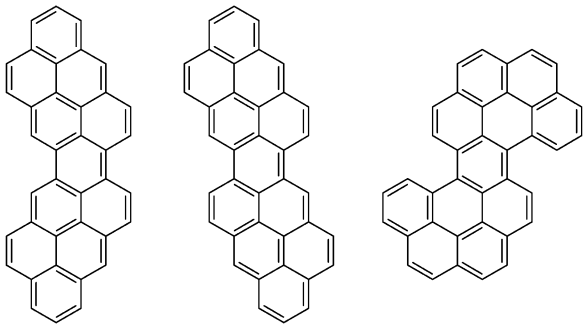

6 **7** **8**

Results and Discussion

The results of semiempirical and HF, DFT, and MP2 ab initio calculations of $C_{38}H_{18}$ undecacyclic non-Kekulé LPAHs **1**, **4**, and **5** were compared with the corresponding results of the following selected isomeric $C_{38}H_{18}$ undecacyclic Kekulé LPAHs: C_{2v}-anthra[2,1,9,8-*klmno*]naphtho[3,2,1,8,7-*vwxyz*]hexaphene (**6**), C_{2h}-dianthra[2,1,9,8-*stuva*:2′,1′,9′,8′-*hijkl*]pentacene (**7**), and C_2-dibenzo[*jk*,*uv*]dinaphtho[2,1,8,7-*defg*:2′,1′,8′,7′-*opqr*]pentacene (**8**).[17] The choice of LPAHs **6**−**8** was based on the following considerations: **6** and **7** are the most stable $C_{38}H_{18}$ products of the *peri*−*peri* reductive coupling of **2** and are planar, like **1**. LPAH **8** is the preferred nonplanar product of the corresponding Clar synthesis and the low valent titanium induced reductive coupling of **2**.[27] It has been known that DFT can be used to probe the aromaticity of large molecular systems, in a cost-effective way, using the different energetic, geometrical, and magnetic criteria of aromaticity.[28] In the present case of **1**, **4**, and **5**, which are diradicals, spin unrestricted wave functions are required for correct description of electronic structure.

Table 1 gives the semiempirical AM1 and PM3 relative heats of formation ($\Delta\Delta H_f°$) of LPAHs **1** and **4**−**8**. Table 2 gives the ab initio HF/6-31G*, B3LYP/STO-3G, B3LYP/6-31G*, B3LYP/6-311G**, and MP2/6-31G*//HF/6-31G* relative energies (ΔE_{Tot}) of LPAHs **1**, **4**, and **5** (spin unrestricted calculations) and **6**−**8** (spin restricted calculations). Note that spin unrestricted treatment of LPAHs **6**−**8** did not lead to solutions with lower energy.

Semiempirical calculations at C.I. = 8 (eight molecular orbitals (MOs) are used in Configuration Interaction calculations) predict triplet **1** to be less stable than **6** by only 86.1 (AM1) and 86.8 (PM3) kJ/mol (Table 1). The triplet states of its isomers **4** and **5** are predicted to be less stable than **6** by 79.4 and 76.6 kJ/mol (AM1) and 81.3 and 84.6 kJ/mol (PM3). This difference in stability between non-Kekulé LPAH **1** and Kekulé LPAH **6** is relatively small, taking into account the different numbers of π-bonds: 18 in **1** and 19 in isomeric **6**. The singlet−triplet gap of concealed non-Kekulé LPAH **1** is negligible at C.I. = 2 ($\Delta\Delta H_f°$ = 0.02 (AM1) and 0.04

(25) (a) Stewart, J. J. P. *J. Comput. Chem.* **1989**, *10*, 221−264. (b) Stewart, J. J. P. *J. Comput.-Aided Mol. Des.* **1990**, *4*, 1−105. (c) Stewart, J. J. P. *MOPAC* 6.00, QCPE 455 **1990**.

(26) Stewart, J. J. P. *MOPAC 93*, Manual Revision Number 2; FUJITSU Limited, **1993**.

(27) Pogodin, S.; Agranat, I. *Org. Lett.* **1999**, *1*, 1387−1390.

(28) De Proft, F.; Geerlings, P. *Chem. Rev.* **2001**, *101*, 1451−1464.

(PM3) kJ/mol) and reaches 2.9 (AM1) and 2.3 (PM3) kJ/mol at C.I. = 8, with the singlet state being more stable. The triplet states of nonconcealed non-Kekulé LPAHs **4** and **5** are significantly more stable than the respective singlet states by 22.2 and 40.4 kJ/mol (AM1) and 19.7 and 39.3 kJ/mol (PM3). It is noted that the results of AM1 and PM3 calculations are very similar. The use of eight MOs for the C.I. calculations seems to be important: C.I. = 2 and 4 do not provide sufficient active space, while C.I. = 6 does not treat correctly partially filled degenerated MOs 82, 83 and 88, 89 of **1** and **4** (MOs 85 and 86 are singly occupied, and MO 87 is the lowest unoccupied MO).

Contrary to the semiempirical results, UHF calculations at 6-31G* basis set (Table 2) predict both the triplet and singlet states of non-Kekulé LPAH **1** to be more stable than Kekulé LPAH **6**: $\Delta E_{\mathrm{Tot}} = -209.6$ kJ/mol (triplet **1**) and −318.2 kJ/mol (singlet **1**). However, the question of reliability of UHF formalism for treatment of diradicals with delocalized unpaired electrons should be born in mind.[29] The severe spin contamination in both triplet ($\langle S^2\rangle = 5.91$) and singlet ($\langle S^2\rangle = 5.59$) wave functions indicates that a single reference UHF determinant is inadequate. Multiconfigurational self-consistent field calculations may be more appropriate for this scenario.[30] Introducing the electron correlation provided by MP2 correction (UMP2/6-31G* single point at UHF/6-31G* geometry) seems to overestimate the energy of the triplet and singlet states of LPAH **1**: $\Delta E_{\mathrm{Tot}} = 767.3$ kJ/mol (triplet **1**) and 798.4 kJ/mol (singlet **1**). It is noted that singlet **1** is more stable than triplet **1** at the UHF level ($\Delta E_{\mathrm{Tot}} = 108.6$ kJ/mol), but triplet **1** is more stable than singlet **1** according to the UMP2 results ($\Delta E_{\mathrm{Tot}} = 31.1$).

The results of the DFT calculations of LPAHs **1**, **4**, and **5** differ from the UHF results and seem to resemble the results of semiempirical calculations. Triplet **1** is less stable than **6** by 87.4 kJ/mol, and singlet **1** is less stable than **6** by 83.8 kJ/mol (at B3LYP/6-31G*). The singlet−triplet gap ($\Delta E_{\mathrm{S-T}}$) is 3.6 kJ/mol in favor of the singlet. Upgrading the basis set to triple split valence 6-311G** raises the relative total energies of the triplet and singlet states of **1** to 90.4 and 86.9 kJ/mol, respectively, and slightly lowers $\Delta E_{\mathrm{S-T}}$ to 3.4 kJ/mol. It is noted that the relative energies of Kekulé LPAHs **7** and **8** increase by 0.1 and 1.0 kJ/mol, respectively, with expanding the basis set from 6-31G* to 6-311G**, whereas for non-Kekulé LPAH **1** the upgrade appears to be more important. The triplets of **4** and **5** are higher in energy than **6** by 63.6 and 80.1 kJ/mol, respectively, but more stable than the triplet **1** by 23.8 and 7.3 kJ/mol, respectively (at B3LYP/6-31G*). The singlet states of **4** and **5** are less stable than the respective triplet states by 12.9 and 18.1 kJ/mol. It should be noted that spin contamination in singlet **1** is still significant ($\langle S^2\rangle = 1.22$ after removing the first spin contaminant, at B3LYP/6-311G** and 1.33 at B3LYP/6-31G*), suggesting not a pure singlet state. The singlet states of **4** and **5** show less degree of spin contamination ($\langle S^2\rangle = 0.61$ and 0.47, respectively, at B3LYP/6-31G*).

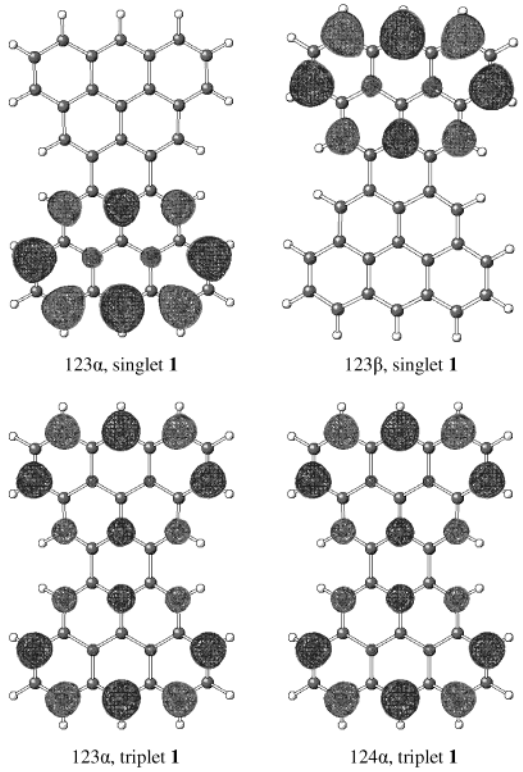

FIGURE 1. The POMOs of concealed non-Kekulé LPAHs **1**: 123α and 123β, singlet **1**; 123α and 124α, triplet **1** (at UB3LYP/6-311G**).

The singlet−triplet gaps in **1** vs **4** and **5** and the violation of Hund's rule in **1** deserve a comment. The prediction of the ground states of non-Kekulé hydrocarbons may be based on Ovchinnikov's formula $S = |n^* - n|/2$, where S is the spin quantum number of the ground state, and n^* and n are, respectively, the number of starred and unstarred carbons.[10,31,32] When $n^* = n$, a singlet ground state ($S = 0$) is expected; when $n^* - n = 2$, a triplet ground state is predicted.[10,31,32] In the case of Clar Goblet (**1**), a concealed non-Kekulé LPAH ($n^* = n$), the ground state should be a singlet. Indeed, in singlet **1**, the partially filled MOs (POMOs) 123α and 123β are disjoint and are confined to different sets of carbon atoms, the upper and the lower benzo[*cd*]pyrenyl subunit, respectively (Figure 1). In triplet **1**, the POMOs 123α and 124α span the same set of carbon atoms. By contrast, in the nonconcealed non-Kekulé LPAHs **4** and **5** ($n^* - n = 2$), the triplets are the ground states. Indeed, in both systems the POMOs of singlet and triplet span a common same set of carbon atoms; and only in triplet the Pauli principle operates to prevent the two nonbonding electrons from simultaneously appearing in the same atomic orbital.[32] The above differences in singlet−triplet gaps between concealed and nonconcealed non-Kekulé hydrocarbons highlight the recognition, due to Hückel, that atomic connectivity is a strong determinant of spin multiplicity.[33]

(29) Borden, W. T.; Davidson, E. R.; Feller, D. *Tetrahedron* **1982**, *38*, 737−739.
(30) *Encyclopedia of Computational Chemistry*; Schleyer, P. v. R., Ed.; Wiley: NewYork, 1998; Vol. 4, p 2665.
(31) Ovchinnikov, A. A. *Theor. Chim. Acta* **1978**, *47*, 297−304.
(32) Borden, W. T. In *Diradicals*; Borden, W. T., Ed.; Wiley: New York, 1982; pp 37−39.
(33) Berson, J. A. *Angew. Chem., Int. Ed. Engl.* **1996**, *35*, 2750−2764.

TABLE 3. Semiempirical Total Atomic Spin Densities at Carbon Atoms of the Triplet State of 1

	AM1 calculations				PM3 calculation			
atom	C.I. = 2	C.I. = 4	C.I. = 6	C.I. = 8	C.I. = 2	C.I. = 4	C.I. = 6	C.I. = 8
C^{1}	0.1242	0.1237	0.1220	0.1201	0.1226	0.1224	0.1211	0.1188
C^{2}	0.0000	0.0001	0.0006	0.0019	0.0000	0.0001	0.0005	0.0018
C^{3}	0.1257	0.1244	0.1241	0.1210	0.1263	0.1251	0.1248	0.1215
C^{3a}	0.0000	0.0001	0.0003	0.0006	0.0000	0.0001	0.0002	0.0006
C^{4}	0.2586	0.2520	0.2527	0.2489	0.2655	0.2589	0.2595	0.2562
C^{17b}	0.0000	0.0020	0.0022	0.0019	0.0000	0.0018	0.0016	0.0017
C^{18}	0.0498	0.0521	0.0526	0.0545	0.0486	0.0508	0.0511	0.0533
C^{18a}	0.0000	0.0007	0.0011	0.0021	0.0000	0.0007	0.0009	0.0020
C^{18b}	0.0264	0.0268	0.0264	0.0259	0.0264	0.0267	0.0262	0.0258
C^{18c}	0.0000	0.0000	0.0017	0.0048	0.0000	0.0000	0.0012	0.0047
C^{18d}	0.0890	0.0880	0.0869	0.0902	0.0867	0.0860	0.0863	0.0881

TABLE 4. Ab Initio Total Atomic Spin Densities at Carbon Atoms of the Triplet State of 1

atom	UHF/6-31G*	UB3LYP/STO-3G	UB3LYP/6-31G*	UB3LYP/6-311G**	UMP2/6-31G*//UHF/6-31G*
C^{1}	0.8776	0.2690	0.2712	0.2677	0.8725
C^{2}	−0.8144	−0.1418	−0.1292	−0.1227	−0.8076
C^{3}	0.8813	0.2801	0.2691	0.2639	0.8773
C^{3a}	−0.8810	−0.1527	−0.1443	−0.1308	−0.8778
C^{4}	0.9600	0.4402	0.4130	0.4010	0.9584
C^{17b}	−0.7414	−0.0720	−0.0705	−0.0679	−0.7339
C^{18}	0.7844	0.1135	0.1106	0.1074	0.7736
C^{18a}	−0.8524	−0.1007	−0.0946	−0.0874	−0.8465
C^{18b}	0.9016	0.0905	0.0810	0.0732	0.8991
C^{18c}	−0.9134	−0.0827	−0.0797	−0.0735	−0.9077
C^{18d}	0.9043	0.1390	0.1476	0.1451	0.9002

Table 3 gives semiempirical AM1 and PM3 total atomic spin densities at the carbon atoms of the triplet **1**. Table 4 gives ab initio UHF/6-31G*, UB3LYP/STO-3G, UB3LYP/6-31G*, UB3LYP/6-311G**, UMP2/6-31G*//UHF/6-31G* total atomic spin densities at carbon atoms of the triplet **1**. All of the above methods show that the spin density is delocalized through alternating positions C^{1} and C^{7}, C^{3} and C^{5}, C^{4}, C^{8} and C^{18}, C^{7b} and C^{18b}, C^{18d}, corresponding to the positions 3 and 9, 5 and 7, 6, 2 and 10, 9^{b} and 11^{c}, 11a of benzo[*cd*]pyrenyl radical **3**, respectively, reaching a maximal value at C^{4}. AM1 and PM3 semiempirical calculations predict the spin density to be localized mainly at C^{4} (0.2562 at C.I. = 8, PM3) and then at C^{1} (0.1188) and C^{3} (0.1215) atoms, while at C^{18}, C^{18b}, and C^{18d} the spin density is significantly lower. Both UHF and UMP2 calculated spin density spreads almost evenly through C^{1}, C^{3}, C^{4}, C^{18}, C^{18b}, and C^{18d} positions, with slight maximum at C^{4}. The DFT spin density pattern resembles the semiempirical one, with the highest spin density at C^{4} (0.4010 at UB3LYP/6-311G**), high spin density at C^{1} (0.2677) and C^{3} (0.2639), and lower spin density at C^{18d} (0.1451), C^{18} (0.1074), and C^{18b} (0.0732). Figure 2 shows the spin density in the triplet **1** (at UB3LYP/6-311G**) and the spin density in doublet **3** (at UB3LYP/6-31G*), respectively. The DFT spin density in triplet **4** is delocalized through all the alternating positions of upper and lower **3** moieties, concentrating mainly at C^{1} (0.3095), C^{3} (0.3076), C^{4} (0.4029), C^{5} (0.3124), C^{7} (0.3145), C^{8} (0.2951), and C^{8b} (0.2911) outer atoms of the lower moiety and C^{11} (0.3151) atom of the upper **3** moiety (at UB3LYP/6-31G*). The distribution of the total atomic spin density through the molecule C_s-**4** is not even: 1.24 of two unpaired electrons concentrate in the lower half of the molecule **4**, while only 0.76 in the upper half. The DFT spin density in triplet **5** is also delocalized through all the alternating positions of both **3** moieties, and the highest spin density is concentrated at C^{1} (0.3253), C^{3} (0.3231), C^{4} (0.4021), C^{5} (0.3215), C^{7} (0.3226), C^{8} (0.2997), and C^{18} (0.3313) atoms of the lower moiety and on C^{17b} (0.3648) of the upper moiety (at UB3LYP/6-31G*). The distribution of the total atomic spin density in C_1-**5** is also uneven: the lower half of the molecule contains 1.30 of two unpaired electrons. It is noted that 1.75 of two unpaired electrons is concentrated in the triangulene[34] (**9**) subunit of **5**, while the rest of the molecule is essentially deprived of unpaired electrons' density. Figure 3 depicts the spin density pattern in obvious non-Kekulé LPAHs **4** and **5**, respectively (at UB3LYP/6-31G*).

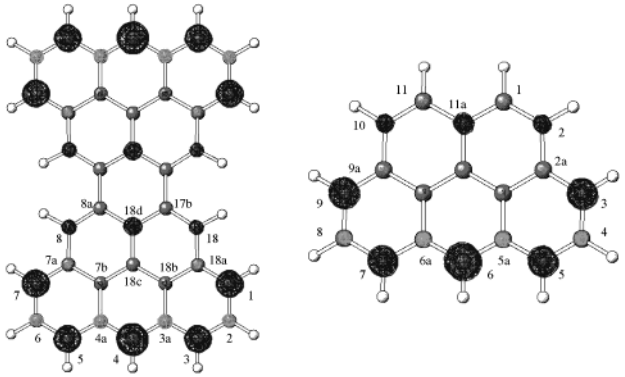

FIGURE 2. The total atomic spin density in triplet **1** (at UB3LYP/6-311G**) and in doublet **3** at UB3LYP/6-31G*).

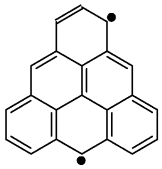

9

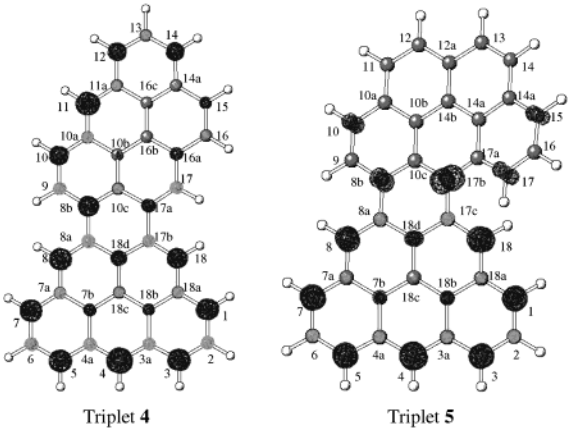

FIGURE 3. The total atomic spin density in triplet **4** and in triplet **5** (at UB3LYP/6-31G*).

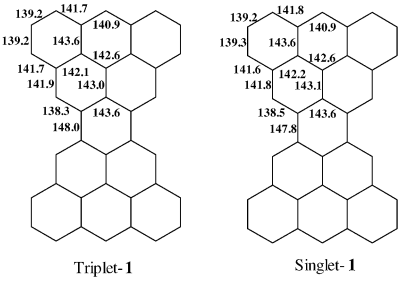

FIGURE 4. The bond lengths in triplet **1** and singlet **1** (at UB3LYP/6-31G*).

The bond lengths in LPAH **1** are found to be in a range expected for aromatic compounds, 138.0−143.3 pm in triplet **1** and 139.7−143.5 pm in singlet **1** (at UHF/6-31G*), and 138.3−143.6 pm in triplet **1** and 138.5−143.6 in singlet **1** (at UB3LYP/6-31G*). The exception is the pair of carbon−carbon bonds in the central aromatic ring that connect two benzo[*cd*]pyrenylidene moieties. These bonds are significantly elongated: 151.1 pm in triplet **1** but only 145.2 pm in singlet **1** (at UHF/6-31G*), and 148.0 pm in triplet **1** and 147.8 in singlet **1** (at UB3LYP/6-31G*). Figure 4 shows the bond lengths in triplet **1** and singlet **1**, at UB3LYP/6-31G*. Similarly, most of the bond lengths in LPAHs **4** and **5** are 136.5−143.8 and 136.6−145.3 in triplet states and 136.8−143.7 and 136.7−144.6 in singlet states, respectively (at UB3LYP/6-31G*). The carbon−carbon bonds connecting the upper and lower part of **4** and **5** are also elongated, 145.7, 146.8 (triplet **4**), 145.1, 145.4 (triplet **5**) and 146.7, 147.5 (singlet **4**), 146.2, 146.3 (singlet **5**). The nonplanar LPAH **5** is also twisted at its central ring, with torsion angles 12.2° (bay region) and 21.4° (cove region) in the triplet state and 13.1° (bay) and 22.2° (cove) in the singlet state (at UB3LYP/6-31G*).

Table 5 gives the charge distribution for triplet **1**, derived from the Mülliken population analysis and the natural population analysis (NPA). At UB3LYP/6-31G*, both methods predict significant charge separation at the periphery of the aromatic system, with high negative charges (−0.13 to −0.34) at C^1, C^2, C^3, C^4, C^{18} and positive charges on the hydrogen atoms. The Mülliken population analysis places positive charges at C^{3a} and C^{18a}, whereas according to the NPA scheme they bear small negative charges. At UB3LYP/6-311G** (the Mülliken population analysis) the charges separation is small, with the highest negative charge (−0.10) located at the centers of each benzo[*cd*]pyrenyliden moiety, on $C.^{18c}$ The charge distribution for singlet **1** is essentially the same as that for triplet **1**. The Mülliken population analysis and NPA predict high negative charges (−0.13 to −0.34) at all of the peripheral aromatic positions bearing hydrogen atoms with the hydrogens being positively charged. The Mülliken scheme also places high positive charges on the peripheral aromatic positions not bearing hydrogen atoms.

TABLE 5. Ab Initio Charge Distribution in the Triplet State of 1

atom	Mülliken population analysis UB3LYP/6-31G*	natural population analysis UB3LYP/6-31G*	Mülliken population analysis UB3LYP/6-311G**
C^1	−0.2205	−0.2004	−0.0780
H^1	0.1296	0.2340	0.0788
C^2	−0.1264	−0.2366	−0.0755
H^2	0.1318	0.2402	0.0927
C^3	−0.2185	−0.1994	−0.0679
H^3	0.1304	0.2332	0.0812
C^{3a}	0.1949	−0.0629	−0.0139
C^4	−0.3278	−0.1629	−0.0197
H^4	0.1329	0.2304	0.0728
C^{17b}	0.0992	−0.0287	−0.0482
C^{18}	−0.3415	−0.1738	0.0271
H^{18}	0.1354	0.2263	0.0771
C^{18a}	0.1801	−0.0544	−0.0523
C^{18b}	−0.0120	−0.0065	−0.0178
C^{18c}	−0.0099	−0.0029	−0.1048
C^{18d}	0.0424	−0.0067	0.0590

SCHEME 1. Homodesmotic Reactions between Singlet 1 and Hydrocarbon 10 (at B3LYP/6-31G*)

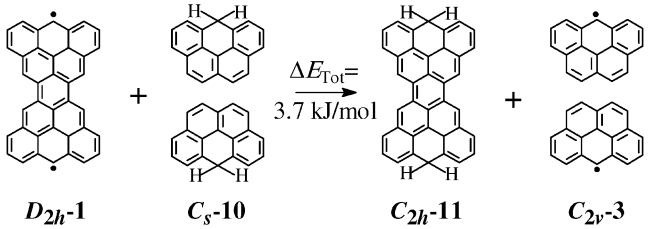

The "communication" between the two benzo[*cd*]pyrenyl radical (**3**) units of **1** may be evaluated by the following homodesmotic reaction involving the reference partially saturated hydrocarbons 6*H*-benzo[*cd*]pyrene (C_{2v}-**10**) and 4,13-dihydro-4*H*,13*H*-diphenaleno[2,1,9,8-*defg*:2′,1′,9′,8′-*opqr*]pentacene (C_{2h}-**11**)[35] (Scheme 1):

$$\text{Singlet-}\mathbf{1} + \mathbf{10} + \mathbf{10} \rightarrow \mathbf{11} + \mathbf{3} + \mathbf{3}$$
$$\Delta E_{\text{Tot}} = 3.7 \text{ kJ/mol (at (U)B3LYP/6-31G*)} \quad (1)$$

This value shows a slightly increased stability of diradical

(34) 2,6,10-Tri-*tert*-butyltriangulene, a ground-state triplet, has recently been detected. Inoue, J.; Fukui, K.; Kubo, T.; Nakazawa, S.; Sato, K.; Shiomi, D.; Morita, Y.; Yamamoto, K.; Takui, T.; Nakasuji, K. *J. Am. Chem. Soc.* **2001**, *123*, 12702−12703.

(35) Planar C_{2v}-**10** (E_{Tot} = −731.30627558 hartree) is a bona fide minimum at B3LYP/6-31G*. Folded C_{2h}-**11** (E_{Tot} = −1460.22999736 hartree) is a transition state at B3LYP/6-31G*, 0.25 kJ/mol lower in energy than the third-order saddle point planar D_{2h}-**11** (E_{Tot} = −1460.22990244 hartree).

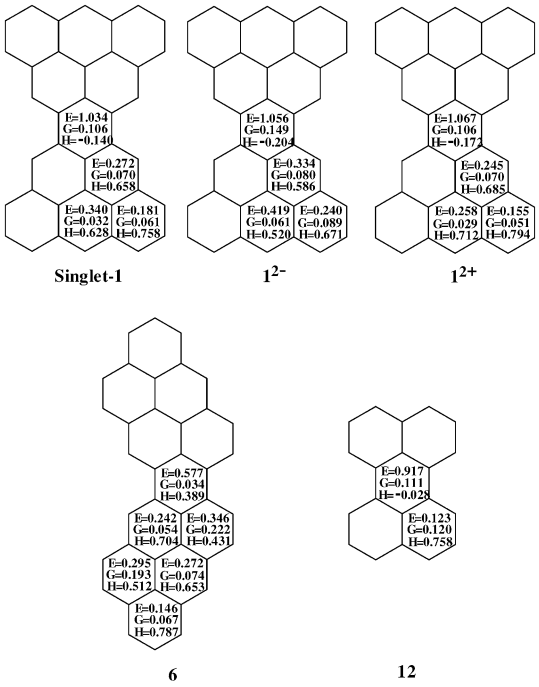

FIGURE 5. HOMA, EN, and GEO terms for singlet **1**, dianion ($\mathbf{1}^{2-}$), dication ($\mathbf{1}^{2+}$), neutral **6**, and neutral **12**.

1 relative to the two monoradicals **3**, thus indicating a communication between the two subunits of **1**.

The aromatic character of non-Kekulé LPAHs **1**, **4**, and **5** could be explored with the harmonic oscillator model of aromaticity (HOMA) index,[36] based on geometric parameters of aromatic species. The HOMA model allows separating the two terms that contribute to a decrease of aromaticity: that due to the bond elongation (EN) and that due to the bond length alternation (GEO).[36] Figure 5 shows HOMA, EN, and GEO terms for singlet **1** and neutral **6**, calculated from the ab initio geometries (at (U)B3LYP/6-31+G*). In both singlet **1** and triplet **1** all of the rings except the central one have a significant aromatic character, with the EN term being the main contributor to the decrease in aromaticity. The central ring of **1** is essentially antiaromatic having negative HOMA index, −0.140 in singlet **1** and −0.172 in triplet **1**, due to the elongated bonds, 148.0 and 143.7 nm in singlet **1** and 148.2 and 143.7 nm in triplet **1**, respectively. For comparison, the HOMA index in the central ring of perylene (**12**), calculated at B3LYP/6-31+G* geometry, is −0.028 (Figure 5). At UB3LYP/6-31G* and at UB3LYP/6-311G** the HOMA indices of the central ring in **1** are −0.092 in singlet and −0.123 in triplet and −0.044 in singlet and −0.091 in triplet, respectively. The GEO term for the central ring is relatively small, pointing to small bond length alternation. By contrast, the HOMA indices of the central rings in triplet **4** and triplet **5** are small but positive, 0.143 and 0.314, respectively, while the remaining rings are aromatic (at B3LYP/6-31G*).

The stability of non-Kekulé LPAH **1** could, in principle, be affected by transforming it to a close-shell[11] species by adding two electrons or removing its two unpaired electrons. Table 6 gives the ab initio spin restricted and

(36) Krygowski, T. M., Cyrański, M. K. *Chem. Rev.* **2001**, *101*, 1385−1419.

TABLE 6. Ab Initio Relative ΔE_{Tot} Energies of Neutral and Charged Species of 1, 3, 6

		symm				UB3LYP/ 6-31G* ΔE_{Tot} (kJ/mol)	UB3LYP/ 6-31+G* ΔE_{Tot} (kJ/mol)
1	**pl**[a]	D_{2h}	T[b]	neutral	M[c]	87.40[e]	90.88[e]
1	**pl**	D_{2h}	S	neutral	M[c]	83.80[e]	84.71[e]
3	**pl**	C_{2v}	D	neutral	M[d]	0.00	0.00
						RB3LYP/ 6-31G*	RB3LYP/ 6-31+G*
1	**pl**	D_{2h}	*S*	dianion	M[d]	20.04[e]	−51.30[e]
1	**pl**	D_{2h}	*S*	dication	M[d]	1383.92[e]	1426.88[e]
3	**pl**	C_{2v}	S	anion	M[d]	−112.61[f]	−149.29[f]
3	**pl**	C_{2v}	T	cation	M[d]	556.68[f]	577.93[f]
6	**pl**	C_{2v}	S	neutral	M[d]	0.00	0.00
6	**pl**	C_{2v}	S	dianion	M[d]	9.00[e]	
6	**pl**	C_{2v}	S	dication	M[c]	1363.32[e]	

[a] **pl**: planar conformation. [b] D: doublet, S: singlet, T: triplet. [c] Minimum (no imaginary frequencies), at B3LYP/6-31G*. [d] Minimum (no imaginary frequencies) at B3LYP/STO-3G and B3LYP/6-31G*. [e] Relative to neutral **6**. [f] Relative to neutral **3**.

SCHEME 2. Homodesmotic Reactions between Singlet 1 and Anion and Cation of 3 (at B3LYP/ 6-31+G*)

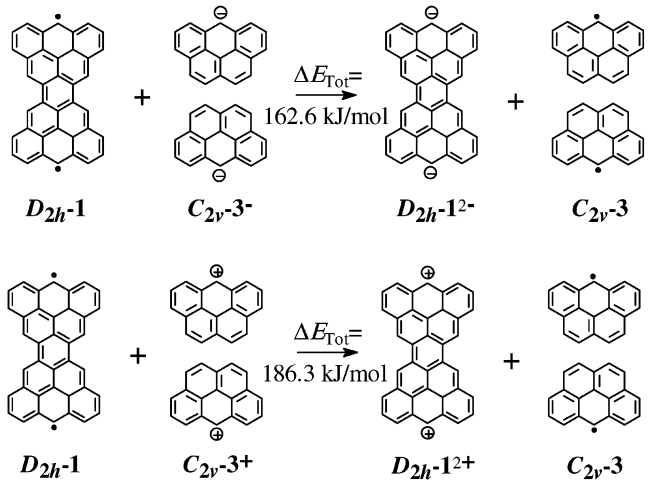

spin unrestricted B3LYP/6-31G* and B3LYP/6-31+G* relative energies (ΔE_{Tot}) of neutral and charged **1**, **3**, and **6**. Adding two electrons to **1** lowers the energy of the species by 136.0 kJ/mol, while subtracting two electrons raises the energy significantly, by 1342.2 kJ/mol (at (U)-B3LYP/6-31+G*). The relative stability of dianion ($\mathbf{1}^{2-}$) and dication ($\mathbf{1}^{2+}$) could be estimated using the following homodesmotic reactions (Scheme 2):

$$\text{Singlet-}\mathbf{1} + \mathbf{3}^{-} + \mathbf{3}^{-} = \mathbf{1}^{2-} + \mathbf{3} + \mathbf{3}$$
$$\Delta E_{Tot} = 162.6 \text{ kJ/mol (at (U)B3LYP/6-31+G*)} \quad (2)$$

$$\text{Singlet-}\mathbf{1} + \mathbf{3}^{+} + \mathbf{3}^{+} = \mathbf{1}^{2+} + \mathbf{3} + \mathbf{3}$$
$$\Delta E_{Tot} = 186.3 \text{ kJ/mol (at (U)B3LYP/6-31+G*)} \quad (3)$$

Both reactions are endothermic, indicating the reduced stability of the dianion and dication of **1**. It should be noted that at B3LYP/6-31G* the dianions of **1** and **6** are bona fide minima. The negative charges in $\mathbf{1}^{2-}$ are concentrated at C^1, C^2, C^3, C^4, C^{18} positions, similarly to the negative charges and spin density in neutral **1**. The

bond lengths are slightly shortened in $\mathbf{1}^{2+}$ as compared to neutral **1**, and slightly elongated in $\mathbf{1}^{2-}$. The HOMA indices for $\mathbf{1}^{2-}$ and $\mathbf{1}^{2+}$ are shown in Figure 5. Transforming **1** into an anion decreases the aromatic character of all the rings, increasing both the bond elongation EN and the bond length alternation GEO terms, while transforming **1** into a cation raises it slightly.

Conclusions

Clar Goblet, the concealed non-Kekulé planar $C_{38}H_{18}$ LPAH D_{2h}-**1** is only 87.4 (triplet) and 83.8 (singlet) kJ/mol (at B3LYP/6-311G**) less stable than planar C_{2v}-**6**, the most stable $C_{38}H_{18}$ products of *peri*−*peri* reductive coupling of **2**. Its nonconcealed planar isomer C_s-**4** is 63.6 (triplet) and 76.5 (singlet) kJ/mol less stable than **6**, while overcrowded C_1-**5** is 80.1 (triplet) and 98.1 (singlet) kJ/mol less stable than **6** (at B3LYP/6-31G*). The singlet state of concealed non-Kekulé **1** is more stable by 3.6 kJ/mol then the triplet state, whereas in nonconcealed non-Kekulé **4** and **5**, triplets were more stable than the corresponding singlets by 12.9 and 18.1 kJ/mol, respectively (at B3LYP/6-31G*). The violation of the Hund's rule in **1** and not in **4** and **5** is consistent to the theory. Spin unrestricted HF and MP2 do not seem to treat those diradicals correctly. The spin density in non-Kekulé LPAHs **1**, **4**, and **5** is delocalized throughout the positions corresponding to active *peri*−*peri* coupling positions of radical anion **2a**, reaching the maximum values at its 5, 6, and 7 positions. The bond lengths in LPAHs **1**, **4**, and **5** are in the range expected for aromatic compounds, with elongated central carbon−carbon bonds. Charges separation is small at UB3LYP/6-311G** level. The relative thermodynamic stability of Clar Goblet (**1**), as reflected in the computational results, does not rule out the possibility of synthesizing it by methods different from the Clar reaction. However, the question of kinetic stability of **1** should not be underestimated. A certain stabilization is evident in the homodesmotic reaction 1, indicating a "communication" between the two benzo[*cd*]-pyrenyl radical units of diradical **1**. Homodesmotic reactions 2 and 3 demonstrate also a decreased stability of $\mathbf{1}^{2-}$ and $\mathbf{1}^{2+}$ compared to that of $\mathbf{3}^{-}$ and $\mathbf{3}^{+}$, respectively. The HOMA indices indicate that the central ring in singlet **1** is essentially antiaromatic having negative HOMA index (−0.140), whereas the HOMA indices of the central rings in triplet **4** and triplet **5** are small but positive.

Acknowledgment. The authors thank Professor W. T. Borden (Department of Chemistry, University of Washington) for fruitful discussions and helpful comments.

Supporting Information Available: Semiempirical AM1 and PM3 heats of formation ($\Delta H_f°$) of LPAHs **1**, **4**−**8**; ab initio HF/6-31G*, B3LYP/STO-3G, B3LYP/6-31G*, B3LYP/6-311G**, MP2/6-31G*//HF/6-31G* total energies (E_{Tot}) of LPAHs **1**, **4**, and **5** (spin unrestricted calculations) and **6**−**8** (spin restricted calculations); ab initio spin restricted and spin unrestricted B3LYP/6-31G* and B3LYP/6-31+G* total energies (E_{Tot}) of neutral and charged **1**, **3**, and **6**; optimized geometries of LPAHs **1**, **4**, **5**, and **6** at AM1 (C.I. = 8) and PM3 (C.I. = 8); optimized geometries of LPAHs **1**, **4**−**8** at (U)HF/6-31G*, (U)-B3LYP/6-31G*, (U)B3LYP/6-311G**; optimized geometries of anion, cation, and neutral species of **1**, **3**, and **6** at (U)B3LYP/6-31G* and (U)B3LYP/6-31+G*; and optimized geometries of **10** and **11** at B3LYP/6-31G*. This material is available free of charge via the Internet at http://pubs.acs.org.

JO026741V